Methods of electron transport in *ab initio* theory of spin stiffness

I. Turek*
Institute of Physics of Materials, Czech Academy of Sciences, Žižkova 22, CZ-616 62 Brno, Czech Republic

J. Kudrnovský† and V. Drchal‡
Institute of Physics, Czech Academy of Sciences, Na Slovance 2, CZ-182 21 Praha 8, Czech Republic

(Received 20 January 2020; accepted 17 March 2020; published 8 April 2020)

We present an *ab initio* theory of the spin-wave stiffness tensor for ordered and disordered itinerant ferromagnets with pair exchange interactions derived from a method of infinitesimal spin rotations. The resulting formula bears an explicit form of a linear-response coefficient which involves one-particle Green's functions and effective velocity operators encountered in a recent theory of electron transport. Application of this approach to ideal metal crystals yields more reliable values of the spin stiffness than traditional ill-converging real-space lattice summations. The formalism can also be combined with the coherent potential approximation for an effective-medium treatment of random alloys, which leads naturally to an inclusion of disorder-induced vertex corrections to the spin stiffness. The calculated concentration dependence of the spin-wave stiffness of random fcc Ni-Fe alloys can be ascribed to a variation of the reciprocal value of alloy magnetization. Calculations for random iron-rich bcc Fe-Al alloys reveal that their spin-wave stiffness is strongly reduced owing to the atomic ordering; this effect takes place due to weakly coupled local magnetic moments of Fe atoms surrounded by a reduced number of Fe nearest neighbors.

DOI: 10.1103/PhysRevB.101.134410

I. INTRODUCTION

The spin stiffness, more specifically also referred to as exchange or spin-wave stiffness, is undoubtedly among the most important properties of itinerant ferromagnets. Its value controls, e.g., the temperature dependence of magnetization at low temperatures, the magnon dispersion law for long wavelengths, and the width of magnetic domain walls. Its reliable experimental or theoretical determination is thus relevant for the whole class of ferromagnetic materials, ranging from pure transition metals [1] to dilute magnetic semiconductors [2].

Existing methods of *ab initio* calculations of magnon spectra and the spin stiffness, as a rule based on the density-functional theory, include a random-phase approximation [3] and techniques dealing with noncollinear magnetic structures, namely, self-consistent total-energy calculations of spin spirals [4–7] and the method of infinitesimal spin rotations [8,9]. The latter approach leads to an effective classical Heisenberg Hamiltonian with isotropic pair exchange interactions between the local magnetic moments; the spin stiffness can then be expressed as a simple real-space lattice sum. However, the asymptotic behavior of the exchange interactions for long interatomic distances was shown to be of the Ruderman-Kittel-Kasuya-Yosida (RKKY) form [10], which leads to an ill-converging behavior of the real-space sum as a function of the cutoff distance. A numerical technique to circumvent this problem was suggested which is based on an artificial damping of the pair interactions and an extrapolation to zero damping [10]. This practical solution seems to be sufficient in certain cases [11,12]; nevertheless, a more fundamental approach to overcome this obstacle would be highly desirable.

Theory and calculations of the spin stiffness for random alloys (substitutionally disordered systems on nonrandom crystalline lattices) face other difficulties. The most direct way to handle the randomness seems to be a generalization of the total-energy spin-spiral calculations using, e.g., the Korringa-Kohn-Rostoker (KKR) multiple-scattering theory and the coherent potential approximation (CPA) [13]. This approach neglects the effects of fluctuating local environments; the same neglect is inherent in the method of infinitesimal spin rotations applied to random alloys in the CPA [14,15]. The local environment effect can be treated in supercell calculations; a study performed for an equiconcentration fcc Ni-Fe alloy proved that the CPA-averaged exchange interactions agree reasonably well with averages from a 16-atom supercell [16]. Another problem related to this topic is the correct CPA average of the pair exchange interactions. The latter involve a product of two one-particle resolvents (Green's functions), so that the proper configuration average should consist of a coherent contribution and the vertex corrections [17]. However, the vertex corrections are typically ignored in existing studies, which is sometimes loosely justified by the so-called vertex-cancellation theorem [18] relevant for interlayer exchange coupling of two ferromagnetic layers separated by a thick nonmagnetic spacer layer. Hence, the role of the vertex corrections in bulk alloy systems deserves more detailed investigation, at least on the CPA level.

*turek@ipm.cz
†kudrnov@fzu.cz
‡drchal@fzu.cz

Besides the mentioned problems in the determination of the exchange interactions of random alloys, the evaluation of magnon spectra of these systems is considered another challenge for the solid-state theory [19]. The formulation of effective-medium approaches is rather sophisticated, and it leads to nontrivial numerical implementation [20,21]. Various brute-force simulations using large supercells have thus been used as alternatives which may be efficient and reliable in a number of cases, including both the spin-wave spectra and values of the spin-wave stiffness [19,21–24]. It was found that the spin stiffness of random diluted ferromagnets is reduced due to the sites without local magnetic moments compared to the value obtained for a clean crystal with nonrandom concentration-weighted exchange interactions of the alloy. This reduction is weak for small concentrations of magnetic vacancies [21], but it becomes appreciable in systems with strong dilution, such as, e.g., Mn-doped GaAs [23,24].

The spin (exchange) stiffness represents one of the micromagnetic parameters of a ferromagnet which describe the energetics and dynamics in cases with magnetization direction slowly varying in space (i.e., the magnetization variations are featured by length scales substantially exceeding the nearest-neighbor interatomic distance). Another micromagnetic parameter, sometimes called spiralization [25], is due to relativistic effects, especially the spin-orbit coupling and the closely related Dzyaloshinskii-Moriya interaction. An *ab initio* relativistic theory of spin stiffness and spiralization for ordered and disordered systems was recently developed within the KKR-CPA technique [26] as an extension of the method of infinitesimal spin rotations [8,9]. For clean crystals, the spiralization was also formulated in terms of the Berry phase of $\mathbf{k}$-vector-dependent Bloch eigenstates of the effective one-electron Hamiltonian [25], i.e., using a concept encountered in the theory of electron transport properties such as the anomalous Hall conductivity [27]. A natural question arises thus in this context, namely, whether the spin stiffness can also be expressed as a linear-response coefficient similar to the conductivity and evaluated by means of techniques employed for electron transport, with applicability to random alloys as well.

From the materials point of view, existing applications of the current *ab initio* techniques for the spin stiffness were focused on pure ferromagnetic $3d$ transition metals (Fe, Co, Ni) [1,5,7,10,28], selected stoichiometric ordered compounds [11,29], random binary and ternary transition-metal alloys [12,13,26,28], and dilute magnetic semiconductors (Mn-doped GaAs) [23,24]. Less attention has been devoted so far to random alloys of transition metals with p elements, such as bcc Fe-M substitutional solid solutions, where $M =$ Be, Al, Si, and Ga. Some of these iron-rich alloys exhibit pronounced magnetoelastic properties (tetragonal magnetostriction) which motivated a number of experimental studies [30,31]. Full assessment of the microscopic origin of this behavior requires fair knowledge of the phonon and magnon spectra. As a rule, the measured magnon spectra of the mentioned bcc Fe-M alloys point to magnon softening due to M alloying [32]. However, a recent *ab initio* study of the spin-wave stiffness of random Fe-Al alloys indicates an opposite concentration trend [21]; this qualitative discrepancy thus deserves closer examination.

The main aim of this study is to present an alternative formalism for the calculation of the spin stiffness in nonrandom and random ferromagnetic systems which employs current techniques of electron transport theory. The developed scheme is then used to address some of the above-mentioned methodological and physical problems. The paper is organized as follows: the theoretical formalism is introduced in Sec. II, the numerical details are listed in Sec. III, and the results are discussed in Sec. IV, including those for pure ferromagnetic $3d$ transition metals (Sec. IV A), for random fcc Ni-Fe alloys (Sec. IV B), and for random bcc Fe-Al alloys (Sec. IV C). Concluding remarks are presented in Sec. V.

II. THEORETICAL FORMALISM

The starting point of our approach to the spin stiffness is the classical Heisenberg Hamiltonian

$$\mathcal{E}(\{\mathbf{e_R}\}) = -\sum_{\mathbf{RR'}} J_{\mathbf{RR'}} \mathbf{e_R} \cdot \mathbf{e_{R'}}, \tag{1}$$

where the indices $\mathbf{R}$ and $\mathbf{R'}$ label the lattice sites, the unit vectors $\mathbf{e_R}$ denote directions of local moments attached to respective lattice sites, and the quantities $J_{\mathbf{RR'}}$ are pair exchange interactions (satisfying $J_{\mathbf{RR}} = 0$ and $J_{\mathbf{RR'}} = J_{\mathbf{R'R}}$). This Hamiltonian is appropriate for ferromagnetic systems that neglect relativistic effects and for local-moment directions deviating only slightly from the ground-state magnetization direction. The latter direction is assumed along the z axis in the following. The spin stiffness is related naturally to energies of spin spirals which are parametrized by a reciprocal space vector $\mathbf{q}$ and a cone angle θ. The spin structure of the spin spiral is then defined explicitly as

$$\mathbf{e_R} = (\sin\theta\cos(\mathbf{q}\cdot\mathbf{R}), \sin\theta\sin(\mathbf{q}\cdot\mathbf{R}), \cos\theta), \tag{2}$$

which yields

$$\mathbf{e_R}\cdot\mathbf{e_{R'}} = \cos^2\theta + \sin^2\theta\cos[\mathbf{q}\cdot(\mathbf{R}-\mathbf{R'})]. \tag{3}$$

The energy of the spin spiral with respect to that of the ferromagnetic ground state is then equal to

$$\delta E(\theta,\mathbf{q}) = \sin^2\theta \sum_{\mathbf{RR'}} J_{\mathbf{RR'}}\{1-\cos[\mathbf{q}\cdot(\mathbf{R}-\mathbf{R'})]\}. \tag{4}$$

This expression in the limit $|\mathbf{q}| = q \to 0$ can be used for a definition of the exchange stiffness relevant, e.g., for energetics of domain walls.

For the spin-wave stiffness related to the magnon spectra and considered in the rest of this paper, one has to include the total spin magnetic moment M of the solid and the quantization of the z component of the total spin operator [5]. This leads to a condition for the small cone angle θ given by

$$2\mu_\mathrm{B} = \delta m_z = M(1-\cos\theta) \approx \tfrac{1}{2}M\theta^2, \tag{5}$$

where the gyromagnetic ratio $g = 2$ for electrons is assumed, μ_B denotes the Bohr magneton, and δm_z is the change in the z component of the total magnetic moment. The last condition

together with Eq. (4) yields the magnon energy

$$E_{\rm mag}(\mathbf{q}) = \frac{4\mu_{\rm B}}{M}\sum_{\mathbf{R}\mathbf{R}'} J_{\mathbf{R}\mathbf{R}'}\{1-\cos[\mathbf{q}\cdot(\mathbf{R}-\mathbf{R}')]\}$$
$$\approx \sum_{\mu\nu} D_{\mu\nu} q_\mu q_\nu, \tag{6}$$

where the approximate relation is valid for small $\mathbf{q}$ vectors with Cartesian components q_μ ($\mu \in \{x, y, z\}$) and where $D_{\mu\nu}$ denotes the spin-wave stiffness tensor. This tensor is explicitly given by

$$D_{\mu\nu} = \frac{2\mu_{\rm B}}{M}\sum_{\mathbf{R}\mathbf{R}'} J_{\mathbf{R}\mathbf{R}'}\big(X^\mu_{\mathbf{R}} - X^\mu_{\mathbf{R}'}\big)\big(X^\nu_{\mathbf{R}} - X^\nu_{\mathbf{R}'}\big), \tag{7}$$

where the symbol $X^\mu_{\mathbf{R}}$ denotes the μ component of the lattice site vector $\mathbf{R}$.

According to the well-known formalism based on infinitesimal spin rotations and the magnetic force theorem [9], the pair exchange interactions $J_{\mathbf{R}\mathbf{R}'}$ can be expressed in terms of the electronic structure of the ferromagnetic ground state as

$$J_{\mathbf{R}\mathbf{R}'} = \frac{i}{8\pi}\int_C {\rm tr}_L\{\Delta_{\mathbf{R}}(z) g^\uparrow_{\mathbf{R}\mathbf{R}'}(z) \Delta_{\mathbf{R}'}(z) g^\downarrow_{\mathbf{R}'\mathbf{R}}(z)\} dz,$$
$$\Delta_{\mathbf{R}}(z) = P^\uparrow_{\mathbf{R}}(z) - P^\downarrow_{\mathbf{R}}(z). \tag{8}$$

In this relation, the trace (${\rm tr}_L$) is taken over the composed orbital index $L = (\ell, m)$, the argument z denotes a complex energy variable, and the complex integration contour C is oriented counterclockwise, with starting and ending points at the Fermi energy $E_{\rm F}$ and containing the whole occupied valence spectrum. The quantities $g^s_{\mathbf{R}\mathbf{R}'}(z)$ abbreviate blocks of matrix elements $g^s_{\mathbf{R}L,\mathbf{R}'L'}(z)$ of one-electron Green's functions $g^s(z)$ in the spin channel s, where $s \in \{\uparrow, \downarrow\}$ is the spin index. The complex integration in Eq. (8) is equivalent to the standard real-energy integration [9,14] owing to analyticity of the integrated function. In this work, we employ the linear muffin-tin orbital (LMTO) method [33–35], in which $g^s(z)$ refers to the auxiliary Green's function defined by

$$g^s(z) = [P^s(z) - S]^{-1}, \tag{9}$$

where $P^s(z)$ denotes the site-diagonal matrix of potential functions and S is the LMTO structure-constant matrix. The site-diagonal blocks $P^s_{\mathbf{R}}(z)$ of the matrices $P^s(z)$ define the energy-dependent local exchange splittings $\Delta_{\mathbf{R}}(z)$ entering the expression for $J_{\mathbf{R}\mathbf{R}'}$ (8); the blocks $\Delta_{\mathbf{R}}(z)$ form a site-diagonal matrix $\Delta(z) = P^\uparrow(z) - P^\downarrow(z)$ to be used in the following. Let us note that the LMTO formalism employed here can be replaced by the KKR formalism, which leads to a replacement of the auxiliary Green's function $g^s(z)$ in the last two equations by the scattering path operator [36,37].

The formulation of a compact expression for the spin-wave stiffness tensor $D_{\mu\nu}$ rests on the definition of coordinate operators X^μ ($\mu \in \{x, y, z\}$), represented by matrices diagonal in the site ($\mathbf{R}$) and orbital (L) indices, given explicitly by

$$X^\mu_{\mathbf{R}L,\mathbf{R}'L'} = \delta_{\mathbf{R}\mathbf{R}'}\delta_{LL'} X^\mu_{\mathbf{R}}. \tag{10}$$

These coordinate operators were introduced in an *ab initio* theory of electron transport [38]. In the present context, one can use them in relations of the type

$$g^s_{\mathbf{R}L,\mathbf{R}'L'}(z)\big(X^\mu_{\mathbf{R}} - X^\mu_{\mathbf{R}'}\big) = [X^\mu, g^s(z)]_{\mathbf{R}L,\mathbf{R}'L'}, \tag{11}$$

where $[A, B] = AB - BA$ is a commutator. The last relation together with Eqs. (7) and (8) leads to the tensor $D_{\mu\nu}$ in the form of a contour integral,

$$D_{\mu\nu} = \frac{\mu_{\rm B}}{2M}\frac{1}{2\pi i}\int_C f_{\mu\nu}(z) dz, \tag{12}$$

with the integrated function $f_{\mu\nu}(z)$ given by

$$f_{\mu\nu} = {\rm Tr}\{\Delta[X^\mu, g^\uparrow]\Delta[X^\nu, g^\downarrow]\}, \tag{13}$$

where all energy arguments (equal z) have been suppressed for brevity and where the trace (Tr) extends over all $\mathbf{R}L$ indices of the whole system. The commutators in the last relation can be rewritten as

$$[X^\mu, g^s] = i g^s v_\mu g^s,$$
$$v_\mu = -i[X^\mu, S], \tag{14}$$

where we introduced the effective velocity operators v_μ that enter the LMTO transport theory as well [38–40]. Relation (14) follows from Eq. (9) and from the site-diagonal nature of the potential functions $P^s(z)$, which implies $[X^\mu, P^s(z)] = 0$. The substitution of Eq. (14) into Eq. (13) and the use of the cyclic property of the trace together with the identity

$$g^\uparrow \Delta g^\downarrow = g^\downarrow \Delta g^\uparrow = g^\downarrow - g^\uparrow \tag{15}$$

yield the final expression for the function $f_{\mu\nu}(z)$, namely,

$$f_{\mu\nu} = -{\rm Tr}\{v_\mu (g^\uparrow - g^\downarrow) v_\nu (g^\uparrow - g^\downarrow)\}, \tag{16}$$

where energy arguments z are omitted. This is the central result of this section.

The final expression for the spin stiffness tensor [see Eqs. (12) and (16)] has the form of a genuine linear-response coefficient suitable for direct numerical evaluation. This calculation requires merely the self-consistent electronic structure of the ferromagnetic ground state as an input for the relevant integrations over the Brillouin zone (BZ) and over the complex energy path (Sec. III). This straightforward procedure should be contrasted with most existing approaches which require (in addition to the self-consistent ferromagnetic ground state) another intermediate step which is numerically quite demanding or delicate. This refers to the method based on the ill-converging real-space lattice summation [10] (where the real-space pair exchange interactions have to be obtained first, followed by an extrapolation with respect to the artificial damping parameter), to the technique employing the spin-spiral calculations [5] (where total energies of the spin spirals for finite $\mathbf{q}$ vectors and cone angles θ have to be obtained first, followed by numerical derivatives), and to the recent KKR approach with reciprocal-space integration [26] (where numerically demanding derivatives of the scattering-path operator with respect to the $\mathbf{k}$-vector components have to be evaluated).

The derived alternative formula for the spin-wave stiffness tensor also deserves further comments. First, in contrast to local exchange splittings entering the previous expressions for this tensor [8,26], the present result contains the nonlocal, spin-independent velocity operators v_μ while all effects of

the exchange splitting are contained in the difference $g^{\uparrow}(z) - g^{\downarrow}(z)$ of the spin-resolved Green's functions. Second, the form of $f_{\mu\nu}(z)$ (16) strongly resembles the Kubo-Greenwood formula for the conductivity tensor $\sigma_{\mu\nu}$ in the LMTO method [38]. The latter is obtained by replacing $g^{\uparrow}(z)$ and $g^{\downarrow}(z)$ in Eq. (16) by $g(E_{\rm F} + i0)$ and $g(E_{\rm F} - i0)$, respectively, i.e., by the retarded and advanced Green's functions at the Fermi energy. Third, this analogy with the theory of electron transport enables one to apply the same techniques of configuration averaging in the CPA also for the spin-wave stiffness tensor of random alloys. In particular, the quantity M in Eq. (12) has to be replaced by the average alloy magnetization, and the CPA average of the Green's function [35,41]

$$\bar{g}^{s}(z) = [\mathcal{P}^{s}(z) - S]^{-1}, \tag{17}$$

where $\mathcal{P}^{s}(z)$ denotes the site-diagonal matrix of coherent potential functions, is used for the average of Eq. (16). This leads to the result

$$\bar{f}_{\mu\nu}(z) = \bar{f}^{\rm coh}_{\mu\nu}(z) + \bar{f}^{\rm VC}_{\mu\nu}(z), \tag{18}$$

where the first term defines the coherent (coh) part, given explicitly by

$$\bar{f}^{\rm coh}_{\mu\nu} = -{\rm Tr}\{v_{\mu}(\bar{g}^{\uparrow} - \bar{g}^{\downarrow})v_{\nu}(\bar{g}^{\uparrow} - \bar{g}^{\downarrow})\}, \tag{19}$$

while the second term in Eq. (18) is the corresponding incoherent part (vertex corrections, VC). Note that this decomposition follows the original approach by Velický [17] owing to the nonrandom effective velocities v_{μ}; the vertex corrections in the present LMTO-CPA formalism have been evaluated according to the Appendix in Ref. [42]. As a direct consequence of the decomposition (18), the spin-wave stiffness tensor of random alloys can also be written as a sum of its coherent and incoherent parts, $D_{\mu\nu} = D^{\rm coh}_{\mu\nu} + D^{\rm VC}_{\mu\nu}$, which represents the complete CPA average. Fourth, the proposed approach is not limited to the LMTO technique, but it is transferable to other electronic structure methods, such as the KKR technique. The effective velocities v_{μ} enter the formalism via the commutator relation, Eq. (14), which involves the diagonal coordinate operators X^{μ}, Eq. (10). The transferability rests on the very simple form of these coordinate operators which reflects the basic starting point of the method of infinitesimal spin rotations [8,9], in which the rotations refer to the whole local magnetic moments at the respective lattice sites.

Finally, the original (canonical) LMTO formalism used in this section can be replaced by its tight-binding (TB) version, in which the potential functions $P^{s}(z)$, the structure-constant matrix S, and the Green's functions $g^{s}(z)$ are replaced by their screened counterparts [35,43,44]. The TB-LMTO technique is advantageous for numerical implementation. It can be proved that the function $f_{\mu\nu}(z)$ (16) and the tensor $D_{\mu\nu}$ (12) are invariant with respect to the TB-LMTO screening transformation. This invariance holds also within the CPA, so that both $D^{\rm coh}_{\mu\nu}$ and $D^{\rm VC}_{\mu\nu}$ are invariant quantities as well. The proof of invariance is omitted here for its similarity to that done in the case of transport properties [40].

III. NUMERICAL IMPLEMENTATION

The developed theory was implemented numerically in a way resembling that employed recently for the so-called Fermi sea contribution to the conductivity tensor in the relativistic TB-LMTO-CPA theory [40]. The self-consistent electronic structure was obtained within the local spin-density approximation (LSDA) and the atomic sphere approximation using the scalar-relativistic *spd* basis [35]. The contour integration in Eq. (12) was performed along a circular path C with a diameter of 1.5 Ry; the numerical integration was done with 20 to 40 complex nodes distributed on the lower half of C. The BZ averages were evaluated by using $\sim 10^8$ **k** vectors for a uniform sampling of one half of the full BZ.

For the sake of a comparison of $D_{\mu\nu}$ calculated from Eq. (12) with results of traditional approaches, we have also applied a procedure based on TB-LMTO-CPA total-energy calculations for spin spirals (2), implemented according to the KKR-CPA technique [13]. The calculations were performed for cubic systems with planar spirals ($\theta = \pi/2$) and **q** vectors along the z axis, $\mathbf{q} = (0, 0, q)$. The spin-wave stiffness, denoted as $D_{\rm sp}$ in the following, was then obtained from a numerical derivative of the total energy as a function of q for $q \to 0$ [5].

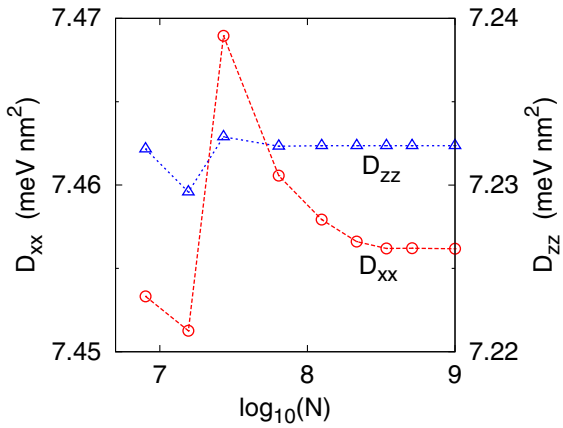

FIG. 1. The calculated spin-wave stiffnesses $D_{xx} = D_{yy}$ (circles, left scale) and D_{zz} (triangles, right scale) for hcp Co as functions of the number N of **k** vectors sampling one half of the first Brillouin zone.

IV. RESULTS AND DISCUSSION

A. Pure transition metals

The numerical aspects of the developed formalism were first examined for pure ferromagnetic $3d$ transition metals: bcc Fe, hcp Co, and fcc Ni. Figure 1 shows the convergence behavior of the spin-wave stiffness tensor for hcp Co. One can see that with the increasing number N of **k** vectors sampling the hcp BZ, both nonzero elements of $D_{\mu\nu}$, namely, $D_{xx} = D_{yy}$ and D_{zz}, exhibit fairly rapid convergence to their limiting values. A similar fast convergence was observed for cubic iron and nickel (not shown here). This convergence property is substantially better than that of the real-space lattice summations (involving the pair exchange interactions) as a function of the cutoff distance $d_{\rm max}$ (see Fig. 2 in Ref. [10]). The reason lies in the typical modest values of $d_{\rm max} < 10a$ used in the lattice summations, where a denotes the lattice parameter. The employed numbers $N > 10^6$ for the BZ sampling (Fig. 1) are

TABLE I. The calculated and experimental values of the spin-wave stiffness D (in meV nm^2) for 3d transition-metal ferromagnets. The values obtained in this work are completed by values calculated previously from spin spirals [5] and from real-space lattice summations [10].

	Calculations			
	This work	Ref. [5]	Ref. [10]	Expt.
Fe	2.73	2.47	2.50	3.3[a]
Co	7.38	5.02	6.63	5.8[b]
Ni	8.01	7.39	7.56	5.3[c]

[a]Reference [45].
[b]Reference [46].
[c]Reference [47].

equivalent to big, but finite, crystals (with periodic boundary conditions) with edge lengths $L \approx N^{1/3}a > 100a$, exceeding thus the cutoff distances $d_{\max}$ by at least one order of magnitude.

Let us note that the convergence problems of the real-space lattice summations are caused by the RKKY-like asymptotic behavior of the pair exchange interactions, leading to their very slow decay for long intersite distances. The new formalism removes the real-space pair interactions completely by using the BZ integrations. Its efficiency is closely related to the lattice Fourier transformation of the TB-LMTO structure constant matrix S, which is the only non-site-diagonal matrix entering the evaluated expression. The spatial range of the matrix S is extremely short, so that, typically, a cutoff to the second or third shell of nearest neighbors is fully sufficient for close-packed lattices such as fcc, bcc, and hcp [43,44]. This property allows one to perform the Fourier transformation very fast and, consequently, to increase the number of the sampling $\mathbf{k}$ vectors substantially.

The converged values of the spin-wave stiffness D for all three metals are summarized in Table I together with values obtained from the spin-spiral calculations [5] and the real-space lattice summations [10] as well as from experiments. The value of D for hcp Co in Table I refers to the isotropic part of $D_{\mu\nu}$, i.e., $D = (2D_{xx} + D_{zz})/3$, whereas the values from both previous calculations [5,10] refer to fcc Co; the experimental value [46] was obtained for the hcp phase. One can observe that all theoretical values reproduce roughly the measured data, with the biggest discrepancy encountered for nickel; for the cubic metals (Fe and Ni), similar values of D were recently obtained by a thorough analysis of results of the KKR multiple-scattering theory [28]. The overestimation of D for Ni by the LSDA calculations can be explained by the well-known overestimation of the exchange splitting which comes out about two times bigger than that from photoemission experiments [48]. A systematic way to achieve better agreement between the theory and the experiment should include effects of electron-electron correlations beyond the LSDA [49]; this task has to be left for future studies.

The calculated tensor $D_{\mu\nu}$ for hcp Co exhibits a small anisotropy featured by $D_{xx} > D_{zz}$ (Fig. 1). However, a recent calculation based on pair exchange interactions up to six nearest neighbors [1] yields an opposite anisotropy ($D_{xx} < D_{zz}$). This fact documents the importance of well-converged values for reliable resolution of subtle details of the spin-wave stiffness tensor. Similarly, the values of D for bcc Fe and fcc Ni obtained in this work (Table I) differ from those based on the real-space lattice summation [10]; the relative difference (below 10% for both metals) points to an uncertainty inherent in the employed regularization procedure of the ill-converging lattice sums [10]. Let us note that pure metals and ordered clean crystals represent the most difficult cases for the lattice-sum approach, whereas random alloys can be treated by this technique with a higher accuracy and efficiency due to the disorder-induced exponential damping of the exchange interactions for large interatomic distances [12].

B. Random fcc Ni-Fe alloys

For the random fcc Ni-Fe alloys, we considered a concentration range up to 60% Fe; the fcc lattice parameter for a given alloy composition was set according to Vegard's law using the experimental atomic (Wigner-Seitz) radii of the pure constituents in their equilibrium structures, $s_{\mathrm{Ni}} = 2.60a_0$ and $s_{\mathrm{Fe}} = 2.66a_0$, where a_0 denotes the Bohr radius. The calculated spin-wave stiffness D is displayed in Fig. 2(a) together with values from the spin-spiral calculations (D_{sp}) and from the experiment [47]. One can see that both calculated quantities, D and D_{sp}, acquire mutually close values and exhibit very similar concentration trends, thus giving confidence in both formalisms and their numerical implementations. Moreover, the calculated values for the permalloy composition $\mathrm{Ni}_{0.8}\mathrm{Fe}_{0.2}$, namely, $D = 5.53$ meV nm^2 and $D_{\mathrm{sp}} = 5.45$ meV nm^2, compare reasonably well with recent KKR values for a $\mathrm{Ni}_{0.81}\mathrm{Fe}_{0.19}$ alloy, which lie in the interval [5.12, 5.63] meV nm^2 depending on the particular approach employed [28]. The experimental stiffness shows also a similar decreasing trend with increasing Fe concentration; however, the measured values are appreciably smaller than the theoretical ones, especially for Ni-rich alloys, which originates in the discrepancy found for pure Ni (see Sec. IV A).

The theoretical results in Fig. 2(a) are in reasonable agreement with those obtained recently from a fully relativistic extension of the method of infinitesimal spin rotations (see Fig. 1 in Ref. [26]). This fact indicates that the spin-orbit interaction has a negligible effect on the spin stiffness in this alloy system and that its omission in the present work cannot be responsible for the existing discrepancy between the theory and experiment for Ni-rich alloys. The decreasing trend of D with increasing Fe content deserves a brief comment as well since attempts to explain similar concentration dependences in binary transition-metal systems appeared rather early [45,50]. Figure 2(b) displays the calculated value of D together with the reciprocal value of the alloy magnetization M, which enters the expressions for D [see Eqs. (7) and (12)]. While the concentration trends of D and $1/M$ differ slightly, the largest part of the variation of the spin-wave stiffness throughout the whole concentration range studied can safely be ascribed to the variation of the alloy magnetization. Finally, we note that the total stiffness D in the fcc Ni-Fe alloys coincides practically with its coherent part while the incoherent part (vertex corrections) is completely negligible in the entire concentration interval (the maximum vertex part is encountered for 60% Fe, where it amounts to about 0.5% of the total D).

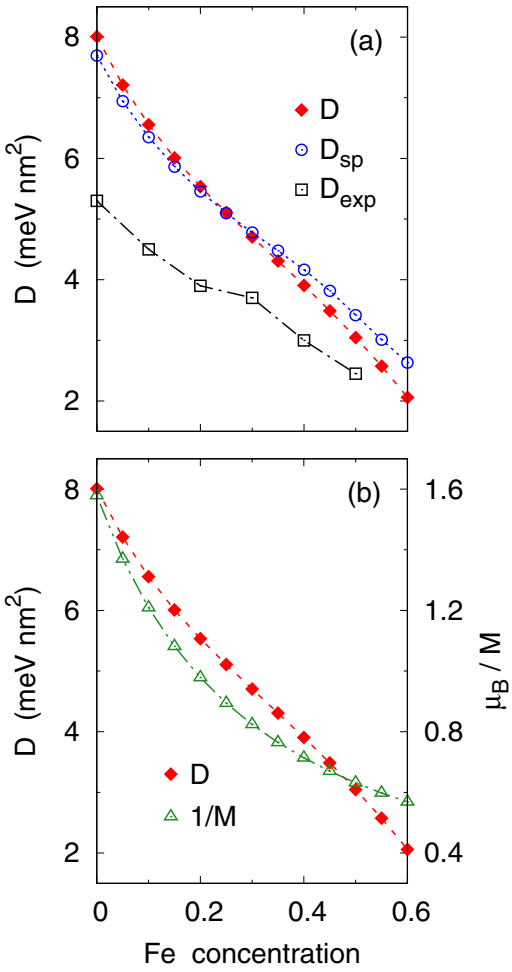

FIG. 2. Concentration dependences of the spin-wave stiffness and the alloy magnetization in a random fcc Ni-Fe alloy: (a) the stiffnesses from Eq. (12) (D, solid diamonds), from spin-spiral calculations (D_{sp}, open circles), and from experiment [47] (D_{exp}, open squares); (b) the stiffness from Eq. (12) (D, solid diamonds, left scale) and the reciprocal value of magnetization per atom ($1/M$, open triangles, right scale).

C. Random bcc Fe-Al alloys

The random bcc Fe-Al alloys were studied for Al concentrations up to 25%; the variation of the bcc lattice parameter with composition was set according to existing experimental data [52,53]. The theoretical values of the spin-wave stiffness are shown in Fig. 3 simultaneously with the experimental points [51] (the measured value for pure iron was taken from Ref. [45]). One reveals a close mutual similarity of both calculated values (D and D_{sp}), which however, differ significantly from the measured values. The measured monotonic decrease of the spin-wave stiffness of bcc Fe due to an alloying by a p element M has been reported not only for M = Al but also for other dopants (M = Be, Ga, Si; see Ref. [32] and references therein). On the theoretical side, the initial decrease of D (up to 5% Al) is changed into an increase for higher Al contents (with a saturation close to 25% Al; see Fig. 3). A nonmonotonic concentration dependence of D has also been calculated by the authors of Ref. [21] with a maximum stiffness around 20% Al.

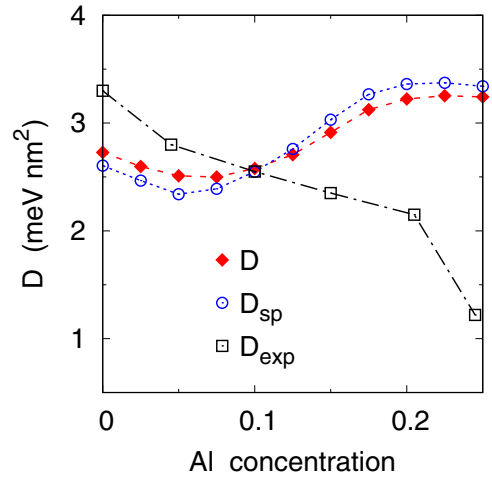

FIG. 3. Concentration dependence of the spin-wave stiffness in a random bcc Fe-Al alloy: the stiffnesses from Eq. (12) (D, solid diamonds), from spin-spiral calculations (D_{sp}, open circles), and from experiment [45,51] (D_{exp}, open squares).

For an explanation of the above discrepancy, one has to consider effects of atomic ordering, pronounced in the Fe-Al alloy especially for higher Al concentrations [54] but neglected in the calculations reported in Ref. [21] as well as in our approach (Fig. 3). As suggested by several authors [32,51,55], the strong reduction of the spin-wave stiffness for the alloy with 25% Al compared to that of pure iron should be ascribed to the $D0_3$ or $B2$ atomic orders. Moreover, theoretical investigation of the atomic short-range order in bcc Fe-Al alloys predicts that the alloys with about 20% Al exhibit a substantial degree of the B2 short-range order when annealed from high temperatures [56,57]. Our theoretical spin-wave stiffness for the stoichiometric Fe_3Al system with the $D0_3$ structure amounts to $D = 1.74$ meV nm^2, which represents a pronounced reduction compared to the calculated value for pure Fe ($D = 2.73$ meV nm^2), but it still remains above the experimental value for alloys with 25% Al (see Fig. 3).

In order to assess the effect of the $B2$ atomic order on the spin-wave stiffness, we have performed calculations for bcc Fe-Al alloys with $B2$ atomic long-range order (LRO). The structure of an $Fe_{1-c}Al_c$ alloy thus contains two simple cubic sublattices with respective compositions given by $Fe_{1-c+u}Al_{c-u}$ and $Fe_{1-c-u}Al_{c+u}$, where c denotes the global Al concentration and u is an auxiliary concentration variable ($0 \leqslant u \leqslant c \leqslant 0.25$). The degree of the $B2$ LRO can then be quantified by the LRO parameter $S = u/c$ ($0 \leqslant S \leqslant 1$); a completely random bcc alloy is given by $S = 0$, whereas the value $S = 1$ refers to the maximum $B2$ LRO. It should be noted that the developed formalism can be directly extended to random systems with a few sublattices within the single-site CPA since the coherent potential function in Eq. (17) is a site-diagonal matrix. The calculated stiffness D for the $Fe_{0.8}Al_{0.2}$ alloy as a function of the LRO parameter S is presented in Fig. 4(a). One can see a monotonic decrease of D with increasing S; the $B2$ LRO thus reduces the stiffness with an efficiency similar to the $D0_3$ order. Since the type and degree of the atomic order in experimentally prepared Fe-Al samples are unknown, we have assumed the maximum $B2$ LRO ($S = 1$)

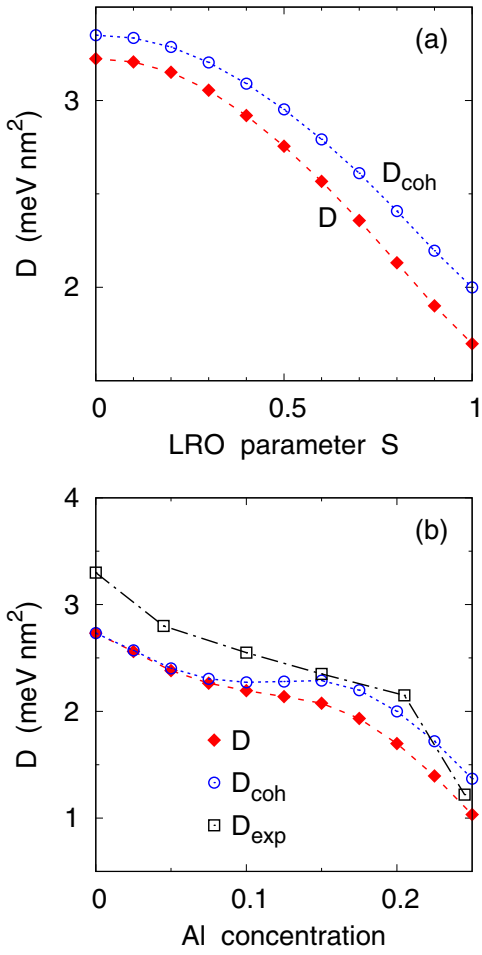

FIG. 4. The spin-wave stiffnesses obtained from Eq. (12) (D, solid diamonds) and its coherent part ($D_{\rm coh}$, open circles) in Fe-Al alloys with $B2$ atomic LRO: (a) in the $Fe_{0.8}Al_{0.2}$ alloy as a function of the LRO parameter S and (b) in Fe-Al alloys with maximum $B2$ LRO as a function of Al concentration together with experimental values [45,51] ($D_{\rm exp}$, open squares).

for each Al concentration and recalculated the composition dependence of the stiffness. As documented in Fig. 4(b), the theoretical values of D reproduce now the measured data in fair agreement, yielding for 25% Al a spin-wave stiffness as low as $D \approx 1$ meV nm^2.

The theoretical results displayed in Fig. 4 include also the coherent part of the spin-wave stiffness which enables one to assess the role of the vertex corrections in this alloy system. One finds that for the completely random bcc $Fe_{0.8}Al_{0.2}$ alloy, the vertex corrections are negative and their magnitude is about 4% of the total stiffness [Fig. 4(a)]. The importance of the vertex corrections increases with increasing Al content and $B2$ LRO; for $Fe_{0.75}Al_{0.25}$ and $S = 1$, the relative magnitude of the incoherent part slightly exceeds 30% of the total D [Fig. 4(b)]. The negative sign and the appreciable magnitude of the vertex corrections bring the theoretical values of D into better agreement with the measured data. A comparison of the role of the incoherent contribution to the spin stiffness in the Fe-Al system to that in the Ni-Fe system (Sec. IV B) reveals a striking analogy to a general rule valid for residual electrical conductivities of random alloys [58]: the vertex corrections are quite small in alloys of transition metals (with dominating d character of electron states at the Fermi energy) but become significant in alloys involving noble and simple metals.

TABLE II. Local quantities of Fe atoms in three different phases (bcc, $D0_3$, $B2$) of the $Fe_{75}Al_{25}$ alloy: the average number of the nearest-neighbor Fe atoms $N_{\rm Fe}$, the relative occurrence w of the particular Fe atom position with respect to all Fe atoms, the local magnetic moment m, and the on-site exchange parameter J^0. For the ordered phases, different sublattices occupied by Fe atoms are denoted in the parentheses.

phase	$N_{\rm Fe}$	w	m ($\mu_{\rm B}$)	J^0 (mRy)
bcc	6	1	2.19	12.6
$D0_3$ (A,C)	4	2/3	1.85	8.0
$D0_3$ (B)	8	1/3	2.37	17.3
$B2$ (A)	4	2/3	1.74	5.6
$B2$ (B)	8	1/3	2.49	14.9

A detailed microscopic explanation of the spin-wave softening due to the atomic ordering in Fe-Al alloys goes beyond the scope of the present work; nevertheless, its possible origin can be estimated from an inspection of various site-resolved quantities of iron atoms. A brief list of such quantities is presented in Table II for the $Fe_{75}Al_{25}$ alloy in three different phases: the random bcc phase, the ordered $D0_3$ structure, and the alloy with the maximum degree of $B2$ LRO. Note that the $D0_3$ structure contains four fcc sublattices, A, B, C, and D, occupied by Fe atoms (A, B, C) and by Al atoms (D), whereby sublattices A and C are mutually equivalent. The $B2$ phase with $S = 1$ consists of two simple cubic sublattices A and B, with the former occupied solely by Fe atoms while the chemical composition of the latter is $Fe_{50}Al_{50}$. The average numbers $N_{\rm Fe}$ of nearest-neighbor Fe atoms of central Fe atoms on different sublattices are displayed in Table II together with their local magnetic moments m and relative occurrences w. The latter quantity is defined with respect to all Fe atoms in the system; that is, w denotes the probability that a randomly chosen Fe atom of the alloy occupies the given sublattice (or any of sublattices A and C in the $D0_3$ phase). The ordering tendencies in the Fe-Al system generally reduce the average number of Fe-Fe nearest neighbors; this reduction is accompanied by a decrease of the local magnetic moments of Fe atoms on the A (and C) sublattice in both ordered alloys that is only partly compensated by an increase of the Fe moments on the B sublattice (see Table II). The ordering induces an even stronger decrease of an on-site exchange parameter J^0 for Fe atoms on the A (and C) sublattice. The on-site exchange parameter is defined in terms of the pair exchange interactions as $J^0_{\mathbf{R}} = \sum_{\mathbf{R}'} J_{\mathbf{R}\mathbf{R}'}$; it reflects the exchange field experienced by the local magnetic moment at site $\mathbf{R}$, and it is evaluated easily from the on-site blocks of the Green's functions by using a well-known sum rule [9,14]. The ordering-induced magnon softening can thus be ascribed to the weakly coupled local moments of Fe atoms featured by a reduced number of Fe nearest neighbors. The validity of this conclusion is probably not confined only to the studied Fe-Al system but can also be extended to other iron-rich alloys with p elements

(e.g., Fe-Si, Fe-Ga) where similar ordering tendencies are encountered as well [54].

V. CONCLUSIONS

In this work, a formulation of the spin-wave stiffness tensor of itinerant ferromagnetic systems has been worked out by employing the concepts and techniques used currently in the theory of electron transport. Application of the developed formalism to clean crystals allows one to overcome convergence problems inherent in real-space lattice summations involving pair exchange interactions. The derived formulas can easily be combined with the CPA for an efficient treatment of substitutionally disordered alloys, which enables one to include the vertex corrections, often neglected in existing calculations of the pair exchange interactions.

The first results of an implementation within the LSDA reproduced successfully previous results of other authors for transition-metal systems; in particular the decreasing trend of the spin-wave stiffness with increasing Fe content in fcc Ni-Fe random alloys was related to the concentration trend of the alloy magnetization. For bcc Fe-Al random alloys, a strong sensitivity of the spin-wave stiffness to the atomic order was proved indispensable for correct reproduction of the measured concentration dependence by the calculations. The two alloy systems studied represent two opposite cases from the viewpoint of the vertex corrections: the latter are negligibly small in the Ni-Fe alloys but appreciable in the Fe-Al alloys. These results thus follow similar findings obtained in the theory of electron transport.

The developed approach to the spin-wave stiffness tensor has been presented in the TB-LMTO method, but it can obviously be implemented in the KKR multiple-scattering theory as well. An open question remains its possible generalization within a relativistic theory of exchange interactions [59,60] and micromagnetic parameters [25,26]; this has to be explored in the future.

ACKNOWLEDGMENT

This work was supported financially by the Czech Science Foundation (Grant No. 18-07172S).

[1] R. Moreno, R. F. L. Evans, S. Khmelevskyi, M. C. Muñoz, R. W. Chantrell, and O. Chubykalo-Fesenko, Phys. Rev. B **94**, 104433 (2016).
[2] P. Němec, V. Novák, N. Tesařová, E. Rozkotová, H. Reichlová, D. Butkovičová, F. Trojánek, K. Olejník, P. Malý, R. P. Campion, B. L. Gallagher, J. Sinova, and T. Jungwirth, Nat. Commun. **4**, 1422 (2013).
[3] J. Callaway, C. S. Wang, and D. G. Laurent, Phys. Rev. B **24**, 6491 (1981).
[4] L. M. Sandratskii, Adv. Phys. **47**, 91 (1998).
[5] N. M. Rosengaard and B. Johansson, Phys. Rev. B **55**, 14975 (1997).
[6] S. V. Halilov, H. Eschrig, A. Y. Perlov, and P. M. Oppeneer, Phys. Rev. B **58**, 293 (1998).
[7] R. H. Brown, D. M. C. Nicholson, X. Wang, and T. C. Schulthess, J. Appl. Phys. **85**, 4830 (1999).
[8] A. I. Liechtenstein, M. I. Katsnelson, and V. A. Gubanov, J. Phys. F **14**, L125 (1984).
[9] A. I. Liechtenstein, M. I. Katsnelson, V. P. Antropov, and V. A. Gubanov, J. Magn. Magn. Mater. **67**, 65 (1987).
[10] M. Pajda, J. Kudrnovský, I. Turek, V. Drchal, and P. Bruno, Phys. Rev. B **64**, 174402 (2001).
[11] S. K. Bose, J. Kudrnovský, V. Drchal, and I. Turek, Phys. Rev. B **82**, 174402 (2010).
[12] O. Šipr, S. Mankovsky, and H. Ebert, Phys. Rev. B **100**, 024435 (2019).
[13] S. Mankovsky, G. H. Fecher, and H. Ebert, Phys. Rev. B **83**, 144401 (2011).
[14] I. Turek, J. Kudrnovský, V. Drchal, and P. Bruno, Philos. Mag. **86**, 1713 (2006).
[15] J. Kudrnovský, V. Drchal, and P. Bruno, Phys. Rev. B **77**, 224422 (2008).
[16] A. V. Ruban, M. I. Katsnelson, W. Olovsson, S. I. Simak, and I. A. Abrikosov, Phys. Rev. B **71**, 054402 (2005).
[17] B. Velický, Phys. Rev. **184**, 614 (1969).
[18] P. Bruno, J. Kudrnovský, V. Drchal, and I. Turek, Phys. Rev. Lett. **76**, 4254 (1996).
[19] P. Buczek, S. Thomas, A. Marmodoro, N. Buczek, X. Zubizarreta, M. Hoffmann, T. Balashov, W. Wulfhekel, K. Zakeri, and A. Ernst, J. Phys.: Condens. Matter **30**, 423001 (2018).
[20] G. Bouzerar and P. Bruno, Phys. Rev. B **66**, 014410 (2002).
[21] P. Buczek, L. M. Sandratskii, N. Buczek, S. Thomas, G. Vignale, and A. Ernst, Phys. Rev. B **94**, 054407 (2016).
[22] B. Skubic, J. Hellsvik, L. Nordström, and O. Eriksson, J. Phys.: Condens. Matter **20**, 315203 (2008).
[23] G. Bouzerar, Europhys. Lett. **79**, 57007 (2007).
[24] I. Turek, J. Kudrnovský, and V. Drchal, Phys. Rev. B **94**, 174447 (2016).
[25] F. Freimuth, S. Blügel, and Y. Mokrousov, J. Phys.: Condens. Matter **26**, 104202 (2014).
[26] S. Mankovsky, S. Polesya, and H. Ebert, Phys. Rev. B **99**, 104427 (2019).
[27] N. Nagaosa, J. Sinova, S. Onoda, A. H. MacDonald, and N. P. Ong, Rev. Mod. Phys. **82**, 1539 (2010).
[28] O. Šipr, S. Mankovsky, and H. Ebert, Phys. Rev. B **101**, 134409 (2020).
[29] J. Kudrnovský, V. Drchal, L. Bergqvist, J. Rusz, I. Turek, B. Újfalussy, and I. Vincze, Phys. Rev. B **90**, 134408 (2014).
[30] J. L. Zarestky, V. O. Garlea, T. A. Lograsso, D. L. Schlagel, and C. Stassis, Phys. Rev. B **72**, 180408(R) (2005).
[31] P. Zhao, J. Cullen, M. Wuttig, H. J. Kang, J. W. Lynn, T. A. Lograsso, and O. Moze, J. Appl. Phys. **99**, 08R101 (2006).
[32] J. L. Zarestky, O. Moze, J. W. Lynn, Y. Chen, T. A. Lograsso, and D. L. Schlagel, Phys. Rev. B **75**, 052406 (2007).
[33] O. K. Andersen, Phys. Rev. B **12**, 3060 (1975).
[34] O. Gunnarsson, O. Jepsen, and O. K. Andersen, Phys. Rev. B **27**, 7144 (1983).
[35] I. Turek, V. Drchal, J. Kudrnovský, M. Šob, and P. Weinberger, *Electronic Structure of Disordered Alloys, Surfaces and Interfaces* (Kluwer, Boston, 1997).

[36] P. Weinberger, *Electron Scattering Theory for Ordered and Disordered Matter* (Clarendon, Oxford, 1990).
[37] J. Zabloudil, R. Hammerling, L. Szunyogh, and P. Weinberger, *Electron Scattering in Solid Matter* (Springer, Berlin, 2005).
[38] I. Turek, J. Kudrnovský, V. Drchal, L. Szunyogh, and P. Weinberger, Phys. Rev. B **65**, 125101 (2002).
[39] I. Turek, J. Kudrnovský, and V. Drchal, Phys. Rev. B **86**, 014405 (2012).
[40] I. Turek, J. Kudrnovský, and V. Drchal, Phys. Rev. B **89**, 064405 (2014).
[41] J. Kudrnovský and V. Drchal, Phys. Rev. B **41**, 7515 (1990).
[42] K. Carva, I. Turek, J. Kudrnovský, and O. Bengone, Phys. Rev. B **73**, 144421 (2006).
[43] O. K. Andersen and O. Jepsen, Phys. Rev. Lett. **53**, 2571 (1984).
[44] O. K. Andersen, Z. Pawlowska, and O. Jepsen, Phys. Rev. B **34**, 5253 (1986).
[45] M. Hatherly, K. Hirakawa, R. D. Lowde, J. F. Mallett, M. W. Stringfellow, and B. H. Torrie, Proc. Phys. Soc. London **84**, 55 (1964).
[46] R. Pauthenet, J. Appl. Phys. **53**, 8187 (1982).
[47] I. Nakai, J. Phys. Soc. Jpn. **52**, 1781 (1983).
[48] D. E. Eastman, F. J. Himpsel, and J. A. Knapp, Phys. Rev. Lett. **44**, 95 (1980).
[49] M. I. Katsnelson and A. I. Lichtenstein, Phys. Rev. B **61**, 8906 (2000).
[50] R. D. Lowde, M. Shimizu, M. W. Stringfellow, and B. H. Torrie, Phys. Rev. Lett. **14**, 698 (1965).
[51] B. Antonini and M. W. Stringfellow, Proc. Phys. Soc. London **89**, 419 (1966).
[52] E. P. Yelsukov, E. V. Voronina, and V. A. Barinov, J. Magn. Magn. Mater. **115**, 271 (1992).
[53] H. Kleykamp and H. Glasbrenner, Z. Metallkd. **88**, 230 (1997).
[54] *Binary Alloy Phase Diagrams*, edited by T. B. Massalski (American Society for Metals, Metals Park, OH, 1986).
[55] E. Frikkee, J. Phys. F **8**, L141 (1978).
[56] J. B. Staunton, M. F. Ling, and D. D. Johnson, J. Phys.: Condens. Matter **9**, 1281 (1997).
[57] J. B. Staunton, S. S. A. Razee, M. F. Ling, D. D. Johnson, and F. J. Pinski, J. Phys. D **31**, 2355 (1998).
[58] J. C. Swihart, W. H. Butler, G. M. Stocks, D. M. Nicholson, and R. C. Ward, Phys. Rev. Lett. **57**, 1181 (1986).
[59] V. P. Antropov and A. I. Liechtenstein, Mater. Res. Soc. Symp. Proc. **253**, 325 (1992).
[60] L. Udvardi, L. Szunyogh, K. Palotás, and P. Weinberger, Phys. Rev. B **68**, 104436 (2003).